APPARATUS DESIGN FOR AN INDEPENDENT MULTIPHASE FLOW RATE METER

Sergio de Paula Pellegrini
Alan Junji Yamaguchi
Flávio Celso Trigo
Raul Gonzalez Lima
Jorge Luis Baliño

Departamento de Engenharia Mecânica, Escola Politécnica, Universidade de São Paulo, Av. Prof. Mello Moraes, 2231, CEP 05508-900, Cidade Universitária, São Paulo, SP, Brazil

sergio.pellegrini@gmail.com, alany@usp.br, trigo.flavio@usp.br, lima.raul@gmail.com, jbalino@usp.br

Sthener Rodrigues Vieira Campos

Petrobras, Centro de Pesquisas e Desenvolvimento Leopoldo Américo Miguez de Mello, CEP 21941-598, Ilha do Fundão, Cidade Universitária, Rio de Janeiro, RJ, Brazil

sthener@petrobras.com.br

Abstract. *This work proposes the design of the sensors for an independent multiphase flow rate meter which shall be composed of two parts: (a) a differential pressure meter and (b) an electrical impedance tomograph test section, consisting of 32 electrodes. The first sub-system shall measure pressure difference and its fluctuations around a restriction in the duct. The second sub-system is the interface with the flow for an electrical impedance tomography device. This meter will be tested with an air-water 2 inch diameter facility at the Multiphase Laboratory at the University of São Paulo. The data obtained from the set of sensors shall be sufficient for the determination of the flow pattern and the estimation of the flow composition and the multiphase flow rate, in a future contribution.*

Keywords: *multiphase flow, air-water flow, flow measurement, electrical impedance tomography, differential pressure*

1. INTRODUCTION

The design of real-time independent multiphase flow rate meters is an open and challenging topic. In the petroleum industry, such a meter would be especially useful for production monitoring – avoiding interruptions in the operation – and fiscal purposes. A typical petroleum multiphase flow is composed of gas, oil, water and other substances at an unknown fraction, requiring the knowledge of flow concentration.

An independent multiphase flow rate meter would require combining information of flow concentration and of pressure difference around a restriction, such as an orifice plate, nozzle or Venturi. All of these systems have calibration curves well established for single phase flows.

The present work presents the conceptual design of an air-water flow rate meter and an experimental setup for testing it. This meter shall be composed of two parts: (a) a differential pressure device and (b) an electrical impedance tomograph, measuring the flow composition. For validation purposes, this system is provided with flow rate meters for each single phase flow, before the mixing, and with a camera for comparison of flow structure observation.

2. LITERATURE

Experimental studies of differential pressure multiphase flow rate meters were carried through in the 1990s (Silva et al., 1991; Fischer, 1994). In these works, Venturi tubes were used to analyze the air-oil-water flows in order to obtain variables that characterize the flow composition, such as the void fraction. Fischer's work concluded that the flow meter could provide reliable results only when the different phases were distributed homogeneously. Thorn et al. (1999) reviewed three-phase flow meters from the literature, all with an uncertainty larger than 5%, and argued that tomographic techniques could be used to narrow the uncertainty and to provide for a stand alone multiphase flow meter.

Without relying on composition meters, two-phase flow meter calibration models were critically reviewed in Bertani et al. (2010). These models introduce a correction for the flow rate, as a single phase calibration curve would over estimate it. Meng et al. (2010) compared different two-phase correlations for Venturi tubes, with a large variation of mean errors depending on the flow regime. Oliveira et al. (2009) compared the accuracy of different correlations for a Venturi tube and an orifice plate, also showing varying mean errors. Paz (2011) developed a virtual metering system for oil and gas field monitoring by using a differential pressure transducer around an orifice plate. The fluid variables are obtained by the operation condition and using a black oil model. Campos et al. (2014) performed multi-rate tests at the Petrobras Urucu oilfield, located at the Amazon florest, using a virtual metering system based on continuous measurements on orifice

plates and batch measurements of fluid composition in separator tests, showing an excellent agreement with oilfield data.

Numerical studies were also implemented since the start of the 2000s. Paladino and Maliska (1999) used CFX 4.4 to study a two-phase flow in a two dimensional model of a Venturi tube and predicted a higher concentration of bubbles near the walls, including the positions of pressure measurement. This result is a recommendation for caution, as the reliability of the measurements is compromised whenever a compressible phase enters the pressure metering system. Indeed, Li et al. (2013) use a swirl inducer flow-conditioning device at the Venturi inlet, to induce a more annular-like flow. Wörner (2003) performed an extensive bibliographic study about the various models for multiphase flow applied to numerical simulation. Imada (2014) carried out a numerical study using the software Fluent with multiphase flows in differential pressure flow meters. The study focused on wet gas flows and concluded that the void fraction is a viable alternative to characterize the flow composition and estimate the multiphase flow rate.

Current industrial multiphase flow meters for oil applications commonly rely on a combination of a Venturi tube and an auxiliary technique, which might be radiation based techniques (Schlumberger Ltd, 2016), ultrasound (Rosen, 2016) or on integral electrical impedance methods (Pietro Fiorentini S.P.A., 2016; Emerson Electric CO., 2016). For other industrial applications, EIT systems for flow composition monitoring are also in the market (Industrial Tomography Systems, 2016; Rocsole LTD, 2016).

Different techniques to measure the void fraction are presented and briefly discussed in Table 1. Two of these are highlighted: the wire mesh and the electrical impedance tomography. The comparative advantage of the wire mesh, of a better space resolution, is a direct consequence of its disadvantage, of intrusiveness. If the device selection was driven by the concern of flow disturbance, wire mesh is a more appropriate technique as the flow is anyway going to be disturbed at the differential pressure meter. However, for situations in which solid particles are carried along with the multiphase flow – typical case within the petroleum industry –, non intrusiveness is desired, for a higher lifetime of the sensor. Thus, Electrical Impedance Tomography (EIT) is selected as the technique for void fraction measurement, in spite of the disadvantage of low spatial resolution, which imposes challenges.

Table 1: Comparative analysis of different methods for void fraction measurement. Based on Silva (2008).

	Advantages	Disadvantages
Computed tomography (X or γ rays)	• High spatial resolution	• Ionizing radiation imposes safety procedures • Complex and expensive hardware
Magnetic resonance imaging	• High spatial resolution • Can provide velocity fields	• Low sampling rate • Complex and expensive hardware
Optical systems (from infrared to ultraviolet)	• High sampling rate • High space resolution • Unexpensive hardware	• Fails in systems with high void fractions • Requires (semi-)transparency of duct wall and fluids
Ultrasound	• High sampling rate • High spatial resolution	• Fails in systems with high void fractions
Integral electrical impedance methods	• High sampling rate • Unexpensive hardware	• Calibration is flow pattern dependent
Electrical Impedance Tomography	• High sampling rate • Unexpensive hardware	• Low spatial resolution
Wire mesh	• Very high sampling rate • Good space resolution • Unexpensive hardware	• Intrusive sensor

EIT provides estimates for the spatial distribution of the phases via a characterization of the electrical properties in the duct, using only measures in electrodes at the duct wall. This configures an inverse, ill-posed and nonlinear problem and the choice of the algorithm used to solve the problem affects considerably the time resolution and the accuracy of the estimates for the phase distribution (Holder, 2005). There seems to be a trade-off between processing speed and precision, depending on the algorithm – issues out of the scope of the present work. Nevertheless, Rocsole LTD (2016) obtains real-time estimates of good space resolution using EIT. An academic work of a partner university of Rocsole reports that $20\,Hz$ is a low frame rate for three-dimensional analysis with 64 electrodes (Seppänen et al., 2007).

In industrial applications, EIT is traditionally divided in two branches: Electrical Resistance Tomography (ERT) and Electrical Capacitance Tomography (ECT). The main differences are the excitation strategy – ERT imposes electric current and ECT imposes electric potential, both measuring the system's electric potential as a response – and the electrical property reconstructed – with ERT estimating conductivity/resistivity and ECT estimating permittivity. Due to the properties of the fluids, an ERT system would be typically used to analyze an air-water flow and an ECT system for an air-oil flow (Silva, 2008). The development of dual modality (ERT/ECT) systems is a recent goal in the field.

An important aspect of a successful implementation of EIT is to cope with the intrinsic challenge of ill-posedness –

i.e., the low spatial resolution. One method to address this challenge is to include, in the estimation problem, information known *a priori* about the multiphase flow under consideration (Kaipio and Somersalo, 2004). However, this prior information on the phase distribution is pattern flow specific (Pellegrini et al., 2016). Thus, it is first necessary to know which flow pattern is present.

Polansky and Wang (2016) used EIT data to identify flow characteristics of annular horizontal and vertical air-water flow using direct proper order decomposition, a method that identifies typical flow structures and instabilities and could potentially be used for flow pattern recognition (Polansky et al., 2015). Using Boolean logic and frequency analysis of the ERT data with 16 electrodes for a air-water flow in a 2 inch diameter duct, Karki et al. (2016) were able to differentiate among bubble, plug, slug, stratified and annular flows with minimum accuracy of 59 %. Dupré et al. (2016) suggest the use of raw ECT data to differentiate the flow regime, with a Fast Fourier Transform to identify intermittent flow and the analysis of the eigen-problem associated with a cross-capacitance matrix, defined among the potential of all electrodes, to differentiate the other flow patterns.

Static pressure can easily be measured in different points and the differential pressure between two measurement points can be analyzed by probability density functions (PDFs) showing different characteristic behaviors for each flow pattern. Most of the investigations reported in the literature were performed in vertical flows, as there is a higher variation of pressure and using sensors capable of measuring higher frequencies (over 50 *Hz*). Matsui (1984) identified four different types of flow patterns (bubble flow, slug-like flow, annular flow and mist flow) using this method in a vertical section using nitrogen gas-water. The works of this area also extend to developing other identification methods, always using differential pressure signals, such as using the wavelet transform (Elperin and Klochko, 2002), elastic maps (Shaban and Tavoularis, 2014a) and machine learning techniques, which may also estimate flow rates (Shaban and Tavoularis, 2014b).

As for the integration of the different measuring techniques, Meng et al. (2010) presented a combined Venturi-ERT system in which the differential pressure information of the first sub-system was complemented with the informations of flow pattern, void fraction and vapor quality, all extracted from the ERT sub-system. On the other extreme, Weatherford (2016) combines information of absolute pressure, temperature, differential pressure over a Venturi tube, velocity obtained with a sonar system, density obtained with a gamma densitometer and water cut obtained with a (near-)infrared sub-system.

3. METHODOLOGY

To accomplish the objective of designing an independent air-water flow rate meter, the methods proposed will be presented in three parts. First, the physical systems that measure the flow will be shown. Next, the strategy for integration of the different measurements will be discussed. Finally, a method for validation is introduced.

3.1 Hardware specifics

The different parts of the measurement system shall be positioned such that the sub-systems which impose the greater disturbance for the flow are more downstream. Care must be taken so that large enough pipe length is allowed to account for entry effects. A scheme of the general layout of the system is shown in Figure 1.

As seen in Figure 1, the meter will be composed of two main sub-systems. On the most downstream part is a differential pressure meter over a restriction. Following on the upstream direction, a piezoresistive pressure and a temperature transducers are positioned. Next, the EIT system is placed. Finally, on the most upstream end, there is a camera.

3.1.1 Differential pressure meter

The first sub-system will consist of a piezoresistive differential pressure sensor over a restriction in the duct, together with absolute pressure and temperature transducers, upstream. The restrictions to be used in the differential meter are the ones defined by the Standard ISO 5167 (ISO, 2003): orifice plates, nozzles and Venturi tubes. The last ones are usually preferred for the low influence on the flow regimes – as orifice plates are more likely to cause the blockage of the fluid phase – and for the lowest pressure loss (Bertani et al., 2010). On the other hand, Venturi tubes impose a larger initial cost (which may be compensated by the lower maintenance costs, as this device is more immune to erosion and internal scaling). Nozzles seem to provide a fair compromise in all factors. The choice of different types of restrictions was made in order to do a comparative study about their effects, in terms of pressure loss and measurement accuracy. Different restriction diameter ratios shall be analyzed, allowing to study varying operation conditions, related to the differential pressure and air and water flow rates.

The operation conditions for the measuring system were determined in accordance with the operation range of the multiphase laboratory. This calculation varies with each type of restriction and its relation with the maximum values of flow rate. In a first approximation, the multiphase flow was considered to be a pseudo-fluid, using the homogeneous model, in such a way that the expansion factor, ϵ, related to compressibility could be neglected.

The range of superficial velocities considered was based upon two conditions: a) the measurement range of the existent

(a) Isometric view

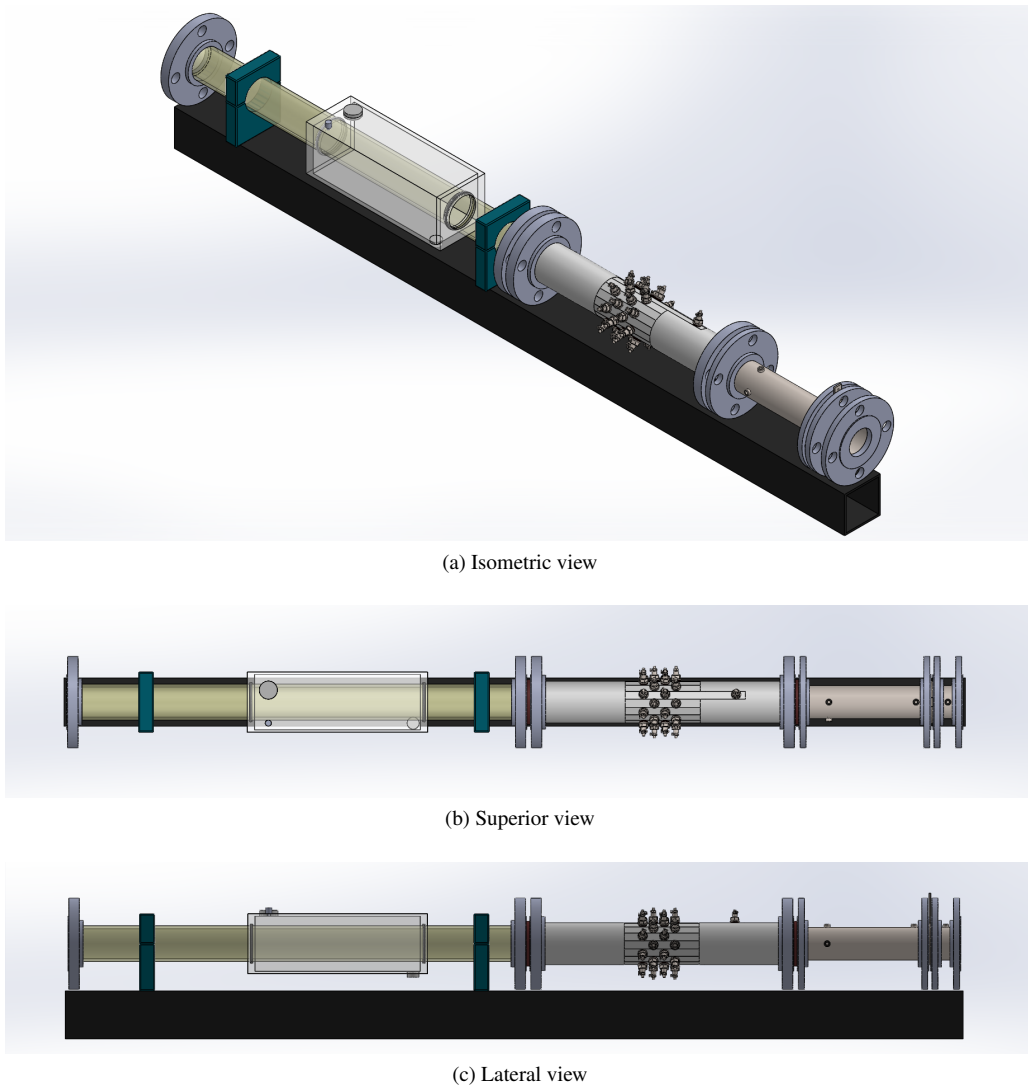
(b) Superior view

(c) Lateral view

Figure 1: General layout for testing setup for independent multiphase flow meter. The visualization section is upstream (left), followed by the tomograph and the absolute pressure, temperature and differential pressure sensors.

flow meters and b) operation range related to real data from the Urucu well production (Imada, 2014). The multiphase laboratory works with maximum air and water superficial velocities of $3 \ m/s$ and $3.4 \ m/s$, respectively, in the 2 inch diameter section. To remain within the the facility bounds, the maximum velocity was defined to be $2 \ m/s$ for air and $1.5 \ m/s$ for water. This latter value tends to fit the experimental data taken from the Urucu well. Using these values and fluid properties on ambient temperature, the discharge coefficient and the differential pressure for different values of diameter ratio, β, were calculated.

With the purpose of obtaining the differential pressure and the discharge coefficient, some other parameters had to be considered, such as the Reynolds number for the equivalent multiphase flow. The homogeneous model was considered to obtain the properties of the mixture: density and viscosity. The viscosity is calculated in the same way as the density (W H McAdams, 1942):

$$\mu_m = \left(\frac{x}{\mu_g} + \frac{1-x}{\mu_l} \right)^{-1} \tag{1}$$

Where x is the mass quality and the indices m, g and l refer respectively to the mixture, gas and liquid. From then on it should be noted that the calculation of the discharge coefficient, C, and its relation with the diameter ratio changes between orifice plates, nozzles and Venturi tubes. In other words the following steps were taken into account in order to define the range of differential pressures:

1. Calculation of the total mass flow considering maximum values of air and water superficial velocity.

2. Homogeneous model as an approximation considering air and water properties at ambient temperature.

3. Determination of the equivalent Reynolds number Re_D.

4. Definition of a range of diameter ratios.

5. Calculation of discharge coefficients for different types of restrictions.

6. Determination of differential pressure values.

The following equation was used to determinate the pressure drop as a function of the other parameters according to the standard ISO5167:2003:

$$\Delta P = \frac{8(1 - \beta^4)}{\rho_m} \left(\frac{W}{C\pi d^2} \right)^2 \tag{2}$$

Where W is the total mass flow and ρ_m is the density of the mixture. The diameter ratio β was varied from 0.5 to 0.75. The orifice plate considered was with flange tappings. For the nozzles the ISA 1932, long radius and Venturi tubes were considered.

The Reader-Harris/Gallagher (Reader-Harris and Sattary, 1996) equation was used to calculate the coefficient discharge for orifice plates:

$$C = 0.5961 + 0.0261\beta^2 - 0.2168\beta^8 + 0.000521 \left(\frac{10^6 \beta}{Re_D} \right)^{0.7} + (0.0188 + 0.0063A)\beta^{3.5} \left(\frac{10^6}{Re_D} \right)^{0.3} +$$
$$(0.043 + 0.08e^{-10L_1} - 0.123e^{-7L_1})(1 - 0.11A)\frac{\beta}{1-\beta^4} -$$
$$0.031(M_2' - 0.8M_2'^{1.1})\beta^{1.3} + 0.011(0.75 - \beta)\left(2.8 - \frac{D}{25.4}\right) \tag{3}$$

Where L_1 and M_2' are quotients related to the upstream and downstream tappings. The discharge coefficient for ISA 1932 and long radius nozzles are calculated as:

$$C = 0.99 - 0.2262\beta^{4.1} - \left(0.00175\beta^2 - 0.0033\beta^{4.15}\right) \left(\frac{10^6}{Re_D} \right) \tag{4}$$

$$C = 0.9965 - 0.00653 \left(\frac{10^6 \beta}{Re_D} \right)^{0.5} \tag{5}$$

For last the Venturi tubes was considered. The equation used was:

$$C = 0.9858 - 0.196\beta^{4.5} \tag{6}$$

A table summarizing the value of ΔP in kPa and discharge coefficient for different types of restrictions together with diameter ratios is shown below. The uncertainty of the discharge coefficient values is lower than 2% in all cases.

Table 2: Differential pressure for different types of restrictions (ISO, 2003).

β	Orifice Plate		ISA 1932		Long Radius		Venturi	
	C_{op}	ΔP_{op}	C_{isa}	ΔP_{isa}	C_{long}	ΔP_{long}	C_{vent}	ΔP_{vent}
0.5	0.610	77.50	0.971	30.59	0.979	30.12	0.977	30.21
0.55	0.614	50.73	0.965	20.51	0.978	19.97	0.972	20.19
0.6	0.618	33.82	0.957	14.11	0.977	13.53	0.966	13.84
0.65	0.624	22.74	0.947	9.87	0.976	9.29	0.958	9.65
0.7	0.632	15.26	0.935	6.96	0.975	6.40	0.946	6.80
0.75	0.642	10.07	0.921	4.90	0.975	4.37	0.932	4.78

From Table 2 the two following differential pressure ranges were defined: 0 to 100 kPa and 0 to 15 kPa. The differential pressure sensors are going to be piezoresistive because these type of sensors have a response time short enough ($< 1\ ms$) to enable the collection of high-frequency data. The absolute pressure range $p(t)$ was defined from 0 to 400 kPa. The temperature range $T(t)$ on the laboratory varies from 0 to $50°C$. All the sensors are planned to have at least 50 Hz of frequency in data collection. The data from the three sensors is intended to be collected using the software Fast Tools from Yokogawa.

3.1.2 Electrical Impedance Tomography

The tomograph excitation strategy is the imposition of electric current, configuring an ERT system. This is justified as the main interest in this study is on air-water flow. The interface with the flow is composed of a set of 32 electrodes, arranged in four cross sections comprised within around $1.5\,D$. An additional electrode is included, to act as a physical ground. The geometrical disposition of the electrodes and the current injection patterns are an important combined issue, addressed for instance by Graham and Adler (2007); Kaipio et al. (2007); Silva et al. (2017). Stainless steel is selected as the material for the electrodes. This is a critical property, as it defines how the system shall age and what are the contact impedances. The duct wall will be made of nylon, for high electrical resistivity and good machinability, besides it being an adequate cheap material for pressure vessels (Ashby, 2011). A final concern for the mechanical design is the sealing of the electrodes. The maximum manometric pressure for the flow in the laboratory is of $300\,kPa$. O-rings were chosen for being the off-the-shelf solution which allows for a simpler manufacturing process for the electrode. The tomography data will be collected with an independent system (Lima et al., 2016).

3.1.3 Flow visualization

An auxiliary measuring system, with a camera, is included in the system for validation purposes. To mitigate distortions related to the curvature of the pipe, a rectangular prism made of acrylic is assembled onto the pipe. This prism should be filled with a fluid of refractive index similar to the acrylic's one. Backlight should also be included. The main constrains for this sub-system are an adequate frame rate and a fair image resolution.

3.2 Integration of sensors

The fusion of sensors measuring quantities of different physical natures is not an evident task. For that purpose, Figure 2 shows a possible scheme for the information flow among the different sensors, determining how the data can be enchained to provide a more reliable estimation for the multiphase flow rate.
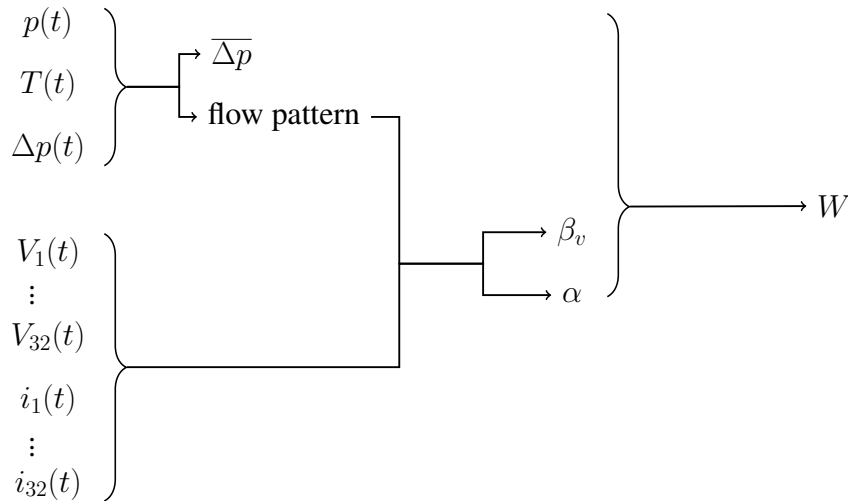

Figure 2: Information flow for independent two-phase flow rate measurement.

The absolute pressure p and the temperature T are important to characterize the thermodynamic state of each fluid. Once a reference thermodynamic state is defined, fluid electric and thermophysical properties can be assessed, either with models or from previous experiments.

The time series of the differential pressure over the restriction $\Delta p(t)$ and of the absolute pressure $p(t)$ can be used to support the determination of the flow pattern. Also, a time average of the differential pressure, $\overline{\Delta p}$, is an important quantity for the determination of the mass flow rate.

As for the ERT system, the time series of the measurements of electric current and potential is combined with the information of which flow pattern is present, to infer the void fraction (α) and the volumetric quality (β_v). The volumetric quality differs from the void fraction as one considers the ratio of the areas (α) while the other considers the ratio of the volumetric flow ratios (β_v).

Finally, the combined set of data is then used to predict a multiphase mass flow rate, according to Paz (2011):

$$W = C_D A_2 \left[\frac{2\,\Delta p}{\left(x + \frac{1-x}{S}\right)\left(\frac{x}{\rho_g} + \frac{1-x}{\rho_l}S\right)(1 - \beta^4)} \right]^{\frac{1}{2}} \tag{7}$$

The previous equation relates the total mass flow rate W to the differential pressure Δp, the cross-sectional area at the restriction A_2, the vapor quality x, the slip ratio S, the specific masses of the air ρ_g and water ρ_l and the diameter ratio β.

The slip ratio can be calculated using the Chisholm correlation (Collier and Thome, 1994):

$$S = \left[1 - x\left(1 - \frac{\rho_l}{\rho_g}\right) \right]^{\frac{1}{2}} \tag{8}$$

The vapor quality can be determined from the average void fraction $\bar{\alpha}$, according to Eq. 9 (Imada, 2014).

$$x = \frac{S\rho_g\bar{\alpha}}{S\rho_g\bar{\alpha} + \rho_l\left(1 - \bar{\alpha}\right)} \tag{9}$$

Imada (2014) defines the average void fraction $\bar{\alpha}$ as a space average of different cross sections, as his study was numerical. For the current analysis, a time average for the ratio of area occupied by the gas at a given section can be calculated from the image estimated with the ERT system.

Synchronization between the data input of both systems is an important property. It is intended to create a shared interface to combine all the data obtained.

3.3 Validation

The meter shall be tested at the Multiphase Laboratory located at the Mechanical Engineering Department of the Polytechnic School of the University of São Paulo (Yamaguchi and Baliño, 2015). The facility consists of a pipeline-riser system of 2 inch diameter pipes, in which air and water can flow. It is intended to test the system initially at the horizontal part of the facility.

The facility pipes have transparent walls, allowing for the visualization of the flow. The camera shall support the validation of the two-phase flow structures identified with the ERT system, at least in a qualitative sense.

Before the mixing of the fluids, the mass flow rate of each phase is measured with single phase meters. Thus, these integral steady state values can be used as a reference for validation of the multiphase flow rate inferred by the independent two-phase flow rate meter.

The expected flow patterns were inferred from the flow pattern map of Taitel and Dukler (1976). The operation range should cover three flow patterns: stratified flow, bubble flow and slug flow.

Table 3 shows the main comparisons which can be made for the parameters of the flow, estimated from the measurements.

Table 3: Validation of the measured parameters.

Parameter	Method 1	Method 2
Void fraction (α)	Flow visualization	Single phase measurements
Mass flow (W)	Single phase measurements	-
Flow pattern	Flow visualization	Flow pattern maps

4. CONCLUSIONS

The design of an independent multiphase flow rate meter was described in this work. This meter is a combination of absolute pressure, temperature, differential pressure over a restriction and ERT sensors. A strategy for the integration of these measurements was briefly shown, leading to estimates for the two-phase flow rate. Technical characteristics and operation ranges were presented, alongside with the planned validation method.

The lack of results at this stage of the work is simply related to the strong dependence of experimental results and measurements of the aparatus which is still in its initial development phase. Future works will cover results and possibly make more pertinent comparisons to other models and even existent meters.

Different types of nozzles shall be tested and compared, for different flow regimes. The two-phase mass flow rate can be predicted with different models. Thus, the accuracy of Eq. 7 could be compared with ISO 2003:5167 and other proposed two-phase correlations.

It is foreseen that processing speed, specially for the flow pattern recognition and the ERT algorithms, might be challenging, and might eventually lead to the determination of the flow rate W with a fixed time delay.

5. ACKNOWLEDGEMENTS

6. REFERENCES

Ashby, M. F. (2011). *Materials selection in mechanical design* (4th ed.). Butterworth-Heinemann.

Bertani, C., M. D. Salve, M. Malandrone, G. Monni, and B. Panella (2010, Sept). State-of-art and selection of techniques in multiphase flow measurement. Technical report, ENEA.

Campos, S. R. V., J. L. Baliño, I. Slobodcicov, D. F. Filho, and E. F. Paz (2014). Orifice plate meter field performance: Formulation and validation in multiphase flow conditions. *Experimental Thermal and Fluid Science 58*, 93–104.

Collier, J. G. and J. R. Thome (1994). *Convective Boiling and Condensation* (3rd ed.). Oxford: Oxford University Press.

Dupré, A., G. Ricciardi, S. Bourennane, and S. Mylvaganam (2016, Sept). Identification of flow regimes using raw eit measurements. In *8th World Congress in Industrial Process Tomography*, Foz do Iguaçú. International Society for Industrial Process Tomography.

Elperin, T. and M. Klochko (2002). Flow regime identification in a two-phase flow using wavelet transform. *Experiments in Fluids 32*, 674–682.

Emerson Electric CO. (Checked in jun/2016). Roxar mpfm 2600. http://www2.emersonprocess.com/en-US/brands/roxar/FlowMetering/meteringsystems/Pages/RoxarMultiphasemeter2600.aspx.

Fischer, C. (1994). Development of a metering system for total mass flow and compositional measurements of multi-phase/multicomponent flows such as oil/water/air mixtures. *Flow Measurement and Instrumentation 5*(1), 31 – 42.

Graham, B. M. and A. Adler (2007). Electrode placement configurations for 3d eit. *Physiological Measurement 28*(7), S29.

Holder, D. S. (Ed.) (2005). *Electrical Impedance Tomography: methods, history and applications*. London: Institute of Physics.

Imada, F. H. J. (2014). Estudo da estrutura multidimensional de escoamentos multifásicos em dispositivos de medição de pressão diferencial. Master's thesis, Universidade de São Paulo, Brazil.

Industrial Tomography Systems (Checked in jun/2016). http://www.itoms.com.

ISO (2003). *ISO Standard 5167 - Measurement of fluid flow by means of pressure differential devices inserted in circular cross-section conduits running full*.

Kaipio, J. and E. Somersalo (2004). *Statistical and Computational Inverse Problems*, Volume 160 of *Applied Mathematical Sciences*. Springer-Verlag New York.

Kaipio, J. P., A. Seppänen, A. Voutilainen, and H. Haario (2007). Optimal current patterns in dynamical electrical impedance tomography imaging. *Inverse Problems 23*(3), 1201.

Karki, B., Y. Faraj, and M. Wang (2016, Sept). Electrical conductivity based flow regime recognition of two-phase flows in horizontal pipeline. In *8th World Congress in Industrial Process Tomography*, Foz do Iguaçú. International Society for Industrial Process Tomography.

Li, Y., W. Yang, C. gang Xie, S. Huang, Z. Wu, D. Tsamakis, and C. Lenn (2013). Gas/oil/water flow measurement by electrical capacitance tomography. *Measurement Science and Technology 24*(7), 074001.

Lima, R. G., A. Luis dos Santos, E. D. L. B. de Camargo, F. Silva de Moura, and T. B. R. Santos (2016). *Signal Processing Architecture for Electrical Tomography Impedance*, pp. 64–67. Singapore: Springer Singapore.

Matsui, G. (1984). Identification of flow regimes in vertical gas-liquid two-phase flow using differential pressure fluctuations. *International Journal of Multiphase Flow 10*, 711–720.

Meng, C., Z. Huang, B. Wang, H. Ji, H. Li, and Y. Yan (2010). Air-water two phase flow measurement using a venturi meter and an electrical resistance tomography sensor. *Flow Measurement and Instrumentation 21*, 268–276.

Oliveira, J. L. G., J. C. Passos, R. Verschaeren, and C. van der Geld (2009). Mass flow rate measurements in gas-liquid flows by means of a venturi or orifice plate coupled to a void fraction sensor. *Experimental Thermal and Fluid Science 33*(2), 253 – 260.

Paladino, E. E. and C. R. Maliska (1999). The effect of the slip velocity on the differential pressure in multiphase venturi flow meters. In *Proceedings of IPC'02, 2002 ASME International Pipeline Conference*.

Paz, E. F. (2011). Sistema baseado em medidor de pressão diferencial para determinação em linha de vazões de produção em poços e petróleo. Master's thesis, Universidade de São Paulo, Brazil.

Pellegrini, S. P., J. L. Baliño, and F. C. Trigo (2016, Sept). Design of a sample-based prior using a phenomenological model for annular flow. In *8th World Congress in Industrial Process Tomography*, Foz do Iguaçú. International Society for Industrial Process Tomography.

Pietro Fiorentini S.P.A. (Checked in jun/2016). Flowatch 3i. http://www.fiorentini.com/ww/en/product/components/mpfm_eng/flowatch3i.

Polansky, J. and M. Wang (2016, Sept). Annular flow pattern recognition using statistical data analyses of electrical

impedance tomography. In *8th World Congress in Industrial Process Tomography*, Foz do Iguaçú. International Society for Industrial Process Tomography.

Polansky, J., M. Wang, and Y. Faraj (2015, Sept). Proper orthogonal decomposition as a technique for identifying multiphase flow regime based on electrical impedance tomography. In *7th International Symposium on Process Tomography*, Dresden. ISPT.

Reader-Harris, M. J. and J. A. Sattary (1996). The orifice plate discharge coefficient equation - the equation for iso 5167-1. *Proceedings of 14th North Sea Flow Measurement Workshop*.

Rocsole LTD (Checked in jun/2016). http://www.rocsole.com/en/technology/.

Rosen (Checked in Nov/2016).

Schlumberger Ltd (Checked in nov/2016). Vx spectra surface multiphase flowmeter. http://www.slb.com/services/characterization/testing/multiphase/spectra.aspx.

Seppänen, A., A. Peltola, L. Heikkinen, J. Kourunen, and J. P. Kaipio (2007). State estimation in process tomography – experimental study in 3d multi-phase flow case. In *5th World Congress on Industrial Process Tomography*.

Shaban, H. and S. Tavoularis (2014a). Identification of flow regime in vertical upward air-water pipe flow using differential pressure signals and elastic maps. *International Journal of Multiphase Flow 61*, 62–72.

Shaban, H. and S. Tavoularis (2014b). Measurement of gas and liquid flow rates in two-phae pipe flows by the application of machine learning techniques to differential pressure signals. *International Journal of Multiphase Flow 67*, 106–117.

Silva, M. J. d. (2008). *Impedance Sensors for Fast Multiphase Flow Measurement and Imaging*. Ph. D. thesis, Technische Universität Dresden.

Silva, O. L., R. G. Lima, T. C. Martins, F. S. de Moura, R. S. Tavares, and M. S. G. Tsuzuki (2017). Influence of current injection pattern and electric potential measurement strategies in electrical impedance tomography. *Control Engineering Practice 58*, 276 – 286.

Silva, S. S., P. Andreussi, and P. D. Marco (1991). Total mass flowrate measurement in multiphase flow by means of a venturi meter. *Multiphase Production*, 145–155.

Taitel, Y. and A. E. Dukler (1976). A model for predicting flow regime transitions in horizontal and near horizontal gás-liquid flow. *American Institute of Chemical Engineers Journal 22*(1), 47–55.

Thorn, R., G. A. Johansen, and E. A. Hammer (1999). Three-phase flow measurements in the offshore oil industry: is there a place for process tomography? In *1st World Congress on Industrial Process Tomography*, Buxton, England.

W H McAdams, W K Woods, L. C. H. (1942). Vaporization inside horizontal tubes ii-benzene-oil mixtures. *Trans. ASME 64*, 193–200.

Weatherford (Checked in nov/2016). Alpha vsrd multiphase flowmeter. http://www.weatherford.com/en/products-services/production/flow-measurement/multiphase-flow-measurement.

Wörner, M. (2003). *A compact introduction to the numerical modeling of multiphase flows*. Forschungszentrum Karlsruhe.

Yamaguchi, A. J. and J. L. Baliño (2015). Experimental study of severe slugging in an air-water pipeline-riser system. In *Proceedings of IV Journeys in Multiphase Flows (JEM2015), 10 p*.

7. RESPONSIBILITY NOTICE

The authors are the only responsible for the printed material included in this paper.